· Article · Advances in Polar Science
doi: 10.13679/j.advps.2018.2.00135 June 2018 Vol. 29 No. 2: 135-143

SHRIMP U-Pb zircon geochronology of granites from Sansom Island, Prydz Bay, East Antarctica

CUI Yingchun[1,2*], LIU Xiaochun[3], LIU Chenguang[1,2*] & LIU Jianhui[4]

[1] Key Laboratory of Marine Sedimentology and Environmental Geology, First Institute of Oceanography, SOA, Qingdao 266061, China;
[2] Laboratory for Marine Geology, Qingdao National Laboratory for Marine Science and Technology, Qingdao 266061, China;
[3] Institute of Geomechanics, Chinese Academy of Geological Sciences, Beijing 100081, China;
[4] Beijing SHRIMP Centre, Institute of Geology, Chinese Academy of Geological Sciences, Beijing 100037, China

Received 14 October 2017; accepted 14 March 2018

Abstract Sansom Island consists of two low nunataks in Sandefjord Bay, a marginal gulf of Prydz Bay, East Antarctica. These nunataks are composed of two kinds of undeformed biotite granites, and these granites have been dated by ion-microprobe U-Pb zircon geochronology. The zircons from these two samples yield SHRIMP zircon U-Pb concordant ages of 516±5 Ma and 495.8±4.2 Ma, respectively. The results indicate that these granites were emplaced in two pulses in the Cambrian, and further demonstrates the Pan-African event that has overprinted this area. The age of *ca*. 516 Ma suggests that the undeformed Sansom Island Granite had a different geological history from the Landing Bluff Granite, which contains deformed granite xenoliths dated at *ca*. 503 Ma, and probably indicates regional variations in the age and intensity of deformation.

Keywords **Granite, Sansom Island, SHRIMP U-Pb zircon geochronology, East Antarctica**

Citation: Cui Y C, Liu X C, Liu C G, et al. SHRIMP U-Pb zircon geochronology of granites from Sansom Island, Prydz Bay, East Antarctica. Adv Polar Sci, 2018, 28 (2): 135-143, doi:10.13679/j.advps.2018.2.00135

1 Introduction

The original geological view of East Antarctica was that it is surrounded by one continuous circum-East Antarctic mobile belt (Moore, 1991), which is commonly referred to as the Grenville-age mobile belt, ranging in age from late Mesoproterozoic to early Neoproterozoic (*ca*.1400−900 Ma) (Fitzsimons, 2000). However, more and more evidence indicates that this supposed Grenville orogenic belt is actually truncated by two younger belts active from the late Neoproterozoic to early Paleozoic (*ca*. 650−500 Ma, also termed Pan-African), namely the Lützow Holm Belt and Prydz Belt (Fitzsimons, 2000; Hensen and Zhou, 1995). The former is the southward continuation of the East African Orogen and marks the final suture of the Mozambique Ocean (Fitzsimons, 2000); while the nature of the latter remains controversial, with one school of thought suggesting that it formed by a collision between an Archaean block and composite terrane (Liu et al., 2014, 2007; Boger et al., 2001; Hensen and Zhou, 1995) and another considering it the result of intraplate orogenesis (Phillips et al., 2009; Wilson et al., 2007). Consequently, both models focus the need for a clear understanding of the geological evolution of this area, in which abundant granites were emplaced during the Pan-African. Since granite records important information related to its generation, ascent and emplacement, these rocks potentially represent a powerful tool to investigate the evolution of this orogenic belt.

Sansom Island, an isolated off-shore island at the eastern edge of the Amery Ice Shelf in Prydz Bay, is completely

* Corresponding authors: E-mail: Cui Yingchun, cuiyingchun@fio.org.cn; Liu Chenguang, lcg@fio.org.cn

composed of granite. The Sansom Island Granite (hereafter called SIG) was traditionally considered to have the similar age to the Landing Bluff Granite (Tingey, 1981) , which has an Rb-Sr whole rock isochron age of 504 ±17 Ma, with an initial $^{87}Sr/^{86}Sr$ ratio of 0.7184±0.0009 (Tingey, 1981). Later, Sheraton et al. (1984) recalculated this age as 493±17 Ma using a different decay constant ($\lambda^{87}Rb=1.42\times10^{-11}$ a^{-1}). These data all have a relatively larger uncertainty, but a more precise U-Pb zircon age of 500 ±4 Ma (Black L Punpublished data) was reported by Tingey (1991). Further constraints on the age of Landing Bluff Granite are provided by the deformed xenoliths within it that have a zircon age of 503±8 Ma (Mikhalsky and Roland, 2007). Although these ages for the Landing Bluff Granite are widely quoted in the literature (e.g. Mikhalsky and Roland, 2007; Tingey, 1991), none of the isotopic data have ever been published. No age data have been reported for the SIG, although its petrology was described by Tingey (1981).

In this contribution, we present the first SHRIMP U-Pb zircon geochronological data for the SIG, in order to define its emplacement age, and we also discuss the geological implications of this age.

2 Geological background

Sansom Island, one of the offshore islands in Sandefjord Bay of Prydz Bay, is mostly covered by ice-snow, with only its peak partly exposed during our expedition. Consequently, it is difficult to clarify its relationship with surrounding geological bodies. Commonly, the SIG, together with the Landing Bluff Granite, is considered as one member of the Landing Bluff Adamellite which occurs in Landing Bluff area and further south to Gillock Island (Tingey, 1981) and intruded high-grade metamorphic country rocks that mainly comprise various orthogneiss and paragneiss units (Liu et al., 2007; Stüwe et al., 1989; Stüwe and Powell, 1989; Tingey, 1981). These country rocks were named the Munro Kerr Gneiss by Tingey (1981) (Figure 1 b), and extend westwards from the Polarforschung Glacier, along the coastal zone and the eastern edge of Amery Ice Shelf, as far as the Reinbolt Hills to the south. The protoliths of these felsic orthogneisses and mafic granulites show some regional variations. For example, in Søstrene Island and the Munro Kerr Mountains area, the mafic protoliths were Nb-enriched arc basalts, while elsewhere the mafic protoliths were volcanic arc basalts (Liu et al., 2014). The felsic orthogneisses all show the characteristics of volcanic arc granites, with distinct differences in geochemistry indicating they formed through different processes (Liu et al., 2014). SHRIMP U-Pb zircon data indicate these felsic and mafic rocks were emplaced over a long period from *ca.*1380 Ma to 1020 Ma (Liu et al., 2014, 2009, 2007).

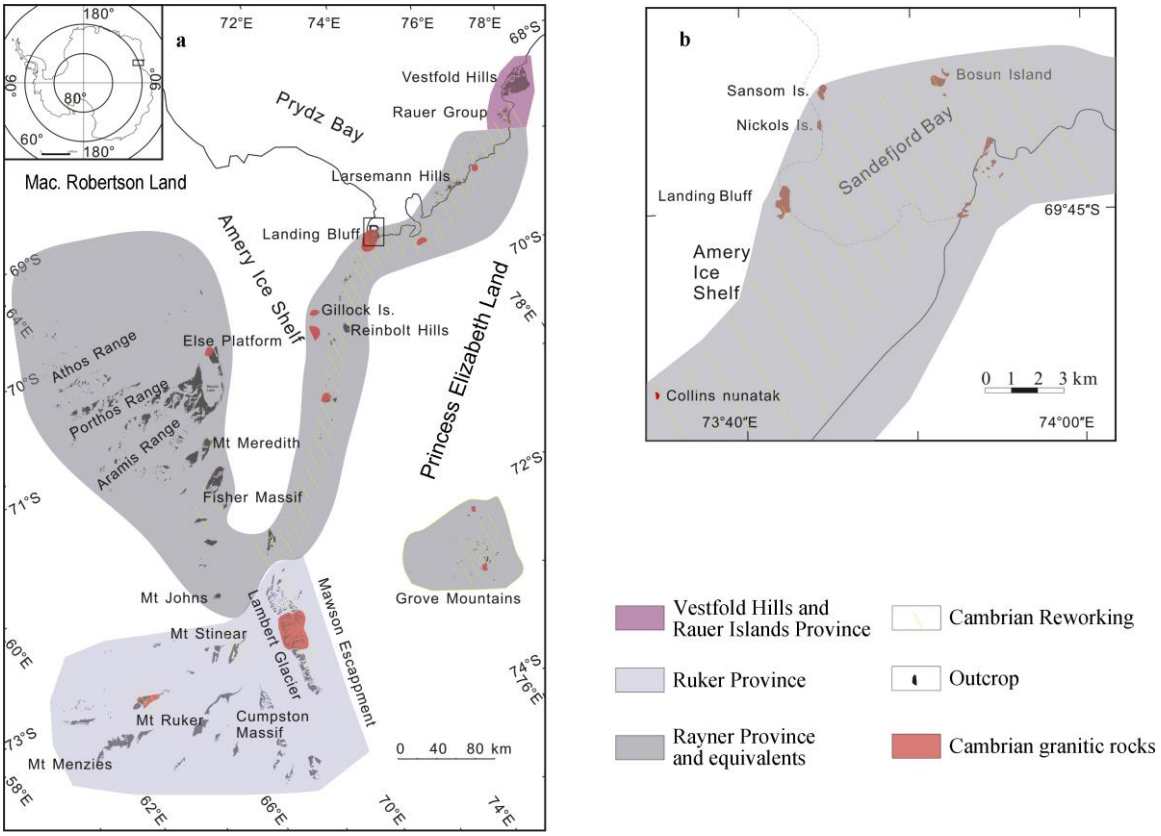

Figure 1 Geological sketch map of Amery Ice Shelf—Lambert Glacier region with inset showing the location of Sansom Island (Modified after Hokada et al. (2016), Liu et al. (2009), Corvino et al. (2008), Li et al. (2007), Mikhalsky and Roland (2007), Carson et al. (1996), Tingey (1981)).

The Munro Kerr Gneiss experienced multiphase metamorphism with events both in the late Mesoproterozoic to early Neoproterozoic and the late Neoproterozoic to early Paleozoic, but the latter metamorphic event is not obviously observed in rocks from the Reinbolt Hills and the Munro Kerr Mountains (Liu et al., 2009). The earlier Grenville-age metamorphism took place at conditions of 8－10 kbar, 900℃; while conditions were *ca.* 4－7 kbar, 650－850℃ during the Pan-African (Hensen and Zhou, 1995).

The deformation history of the Munro Kerr gneiss is poorly constrained. Stüwe and Powell (1989) described the different deformation styles in the Munro Kerr Mountains area, and Nichols and Berry (1991) reported three pervasive deformation phases and two late post-metamorphic deformation phases in the Reinbolt Hills. The age of different deformation phases in the Reinbolt Hills was investigated by Liu et al. (2011). Penetrative tectonic fabrics are lacking in Jennings Promontory (Nichols and Berry, 1991).

2 Methods

2.1 SHRIMP U-Pb

Zircons were separated from the crushed granite samples using conventional techniques (sieving, magnetic separation, heavy liquids and hand picking). About 200 representative zircon grains for each sample were selected by hand-picking, and then mounted in an epoxy disc together with the Temora zircon standard for U-Pb age calibration. Zircon grains were sectioned nearly in half and then polished, in order to expose all of their microgrowth layers. The mount was gold coated, and cathodoluminescence (CL) images of zircon grains were taken using the scanning electron microscope, to characterize the zircon internal structures.

Zircon U-Pb isotopic analyses were carried out using the SHRIMP II sensitive high resolution ion microprobe at the Beijing SHRIMP Centre, Chinese Academy of Geological Sciences. The analytical procedures followed those reported by Williams (1998). A primary ion beam of no more than 4 nA and 23 μm spot size was used. Furthermore, to remove surface contamination, the primary beam was rastered across the sample surface for 2 min before each analysis. Mass resolution was *ca.* 6000 at 1% peak height. Five scans were made in each analysis set, with each scan comprising measurements of the isotope species $^{196}Zr_2O$ (2 s), ^{204}Pb (10 s), ^{206}Pb (20 s), ^{207}Pb (20 s), ^{208}Pb (10 s), $^{238}U^+$ (5 s), ^{248}ThO (2 s) and ^{254}UO (2 s), together with background. The measured U/Pb ratios were calibrated relative to Temora reference zircon (416.75±0.24 Ma; Black et al., 2003), which was measured after every two or three unknown spot analyses. Common Pb correction was carried out using the measured non-radiogenic ^{204}Pb using the Pb evolution model suggested by Stacey and Kramers (1975). The data were reduced using the SQUID 1.03 program (Ludwig, 2001), and the concordia diagrams were plotted using the software ISOPLOT 3.23 (Ludwig, 2003). Uncertainties in the measured isotopic ratios are denoted at one sigma level, however uncertainties for the weighted mean ages are given at 95% confidence level. Here, $^{206}Pb/^{238}U$ ages are presented for zircons in the text, and the analytical data are listed in Table 1.

2.2 Field relationships, petrography and mineralogy

Two granite samples were collected when the helicopter refueled at the Sansom Island fuel base during the 31st Chinese National Antarctic Research Expedition (CHINARE) in the 2014/2015 season. No deformation structures were observed within these two specimens. Sample SI01-1 is a pale pink megacrystic granite with abundant flesh-red, medium-coarse grained K-feldspar crystals (Figure 2a). These euhedral K-feldspar phenocrysts range from 6 mm to 55 mm in size, but they show no obvious zoning. Plagioclase occurs as smaller, cream white grains between the K-feldspar crystals, ranging from 2 mm to 11mm in size. The quartz in this sample occurs as crystal clusters between the K-feldspar crystals, as biotite does. Sample SI01-2 is grey in colour, and its principal minerals are plagioclase, K-feldspar, quartz and biotite (Figure 2b). The euhedral cream white plagioclase phenocrysts range from less than 1 mm to 42 mm in size.

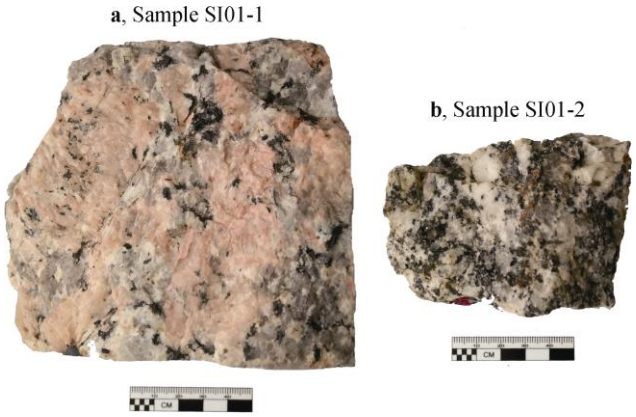

Figure 2 Photoes of samples SI01-1 and SI01-2.

3 Results

3.1 SHRIMP U-Pb geochronology of sample SI01-1

The zircons in this rock have euhedral and anhedral shapes (Figure 3a). They have grain sizes ranging from *ca.* 100 to 500 μm. Most zircons exhibit oscillatory zoning or sector zoning in CL images. While some grains have evidence for a local intermediate stage of resorption, their overall morphology indicates that they were crystallized from magma.

Table 1 SHRIMP U-Pb zircon results for samples SI01-1 and SI01-2, granite from Sansom Island, Prydz Bay

Spot	U /ppm	Th /ppm	$^{232}Th/^{238}U$	$^{206}Pb^*$ /ppm	$^{206}Pb_c$/%	(1)$^{206}Pb/^{238}U$ Age/Ma	(1)$^{207}Pb/^{206}Pb$ Age/Ma	(1)$^{208}Pb/^{232}Th$ Age/Ma	Discordant/%	Total $^{238}U/^{206}Pb$ %	Total $^{207}Pb/^{206}Pb$ %	(1) $^{238}U/^{206}Pb^*$ %	(1) $^{207}Pb^*/^{206}Pb^*$ %	(1) $^{207}Pb^*/^{235}U$ %	(1) $^{206}Pb^*/^{238}U$ %	Errors
SI011																
SI011-1.1	385	468	1.26	25.5	0.15	478.9±8.5	482±64	489±11	1	12.95±1.8	0.05800±1.9	12.97±1.8	0.05680±2.9	0.604±3.4	0.0771±1.8	0.537
SI011-2.1	344	557	1.68	23.7	0.30	497.2±8.8	421±59	494±11	–18	12.43±1.8	0.05760±1.8	12.47±1.8	0.05520±2.6	0.610±3.2	0.0802±1.8	0.575
SI011-3.1	733	744	1.05	50.9	0.13	500.2±8.6	530±28	486±27	6	12.38±1.8	0.05905±1.2	12.39±1.8	0.05801±1.3	0.645±2.2	0.0807±1.8	0.811
SI011-4.1	1418	464	0.34	96.0	0.09	488.8±8.3	492±24	487±13	1	12.68±1.8	0.05773±0.95	12.69±1.8	0.05702±1.1	0.619±2.1	0.0788±1.8	0.848
SI011-5.1	754	640	0.88	51.9	—	497.1±8.6	506±28	507±11	2	12.48±1.8	0.05720±1.3	12.48±1.8	0.05739±1.3	0.634±2.2	0.0802±1.8	0.814
SI011-6.1	104	178	1.77	7.04	—	491.2±9.7	589±66	488±14	17	12.68±2.1	0.05650±3.2	12.63±2.1	0.05960±3.0	0.651±3.7	0.0792±2.1	0.562
SI011-7.1	106	185	1.81	7.07	—	485.5±9.8	560±97	505±14	13	12.83±2.1	0.05570±3.4	12.78±2.1	0.05880±4.5	0.634±4.9	0.0782±2.1	0.427
SI011-8.1	1473	606	0.43	103.0	0.04	502.6±8.6	537±20	497±10	6	12.33±1.8	0.05852±0.89	12.33±1.8	0.05820±0.9	0.651±2.0	0.0811±1.8	0.893
SI011-9.1	441	1151	2.70	31.2	0.17	508.8±9.0	588±53	522±10	14	12.16±1.8	0.06094±1.6	12.18±1.8	0.05960±2.4	0.675±3.1	0.0821±1.8	0.602
SI011-10.1	384	484	1.30	27.0	0.82	502.4±9.1	537±86	506±16	7	12.24±1.9	0.06480±1.7	12.34±1.9	0.05820±3.9	0.650±4.4	0.0810±1.9	0.430
SI011-10.2	304	439	1.49	20.8	0.28	493.2±8.9	422±65	495±11	–17	12.54±1.9	0.05750±2.0	12.58±1.9	0.05520±2.9	0.606±3.5	0.0795±1.9	0.540
SI011-11.1	881	280	0.33	59.4	0.04	486.8±8.4	528±27	482±11	8	12.74±1.8	0.05827±1.1	12.75±1.8	0.05796±1.2	0.627±2.2	0.0784±1.8	0.824
SI011-12.1	307	535	1.80	21.4	—	503.3±9.1	667±39	516±11	25	12.35±1.9	0.05940±1.9	12.32±1.9	0.06180±1.8	0.692±2.6	0.0812±1.9	0.717
SI011-13.1	413	575	1.44	30.2	0.45	525.1±9.7	390±66	517±12	–34	11.73±1.9	0.05812±1.6	11.78±1.9	0.05450±2.9	0.637±3.5	0.0849±1.9	0.550
SI011-14.1	1215	477	0.41	83.1	—	494.0±8.5	512±26	493±11	4	12.57±1.8	0.05697±1.1	12.56±1.8	0.05753±1.2	0.632±2.2	0.0796±1.8	0.833
SI011-15.1	706	492	0.72	48.9	0.08	499.3±8.7	488±40	498±11	–2	12.41±1.8	0.05755±1.3	12.42±1.8	0.05690±1.8	0.632±2.6	0.0805±1.8	0.712
SI011-16.1	345	593	1.77	24.0	—	501.7±9.4	544±41	510±11	8	12.36±1.9	0.05800±1.8	12.36±1.9	0.05840±1.9	0.652±2.7	0.0809±1.9	0.722
SI011-17.1	336	601	1.85	23.3	0.35	498.4±9.0	342±57	502±11	–46	12.40±1.9	0.05620±1.9	12.44±1.9	0.05330±2.5	0.591±3.1	0.0804±1.9	0.599
SI012																
SI012-1.1	416	421	1.05	30.0	—	520.7± 9.2	544±40	524±11	4	11.90±1.8	0.05721±1.4	11.89±1.8	0.05840±1.8	0.677±2.6	0.0841±1.8	0.710
SI012-2.1	111	208	1.94	8.24	—	538.0±10	484±69	529±17	–11	11.56±2.0	0.05260±3.4	11.50±2.0	0.05680±3.1	0.681±3.7	0.0870±2.0	0.546
SI012-3.1	81	175	2.23	5.68	0.15	505.0±11	351±180	507±15	–44	12.25±2.1	0.05480±3.3	12.27±2.2	0.05350±7.9	0.602±8.2	0.0815±2.2	0.263
SI012-4.1	500	298	0.62	35.6	—	513.2± 9.0	534± 29	514±11	4	12.07±1.8	0.05781±1.3	12.07±1.8	0.05810±1.3	0.664±2.3	0.0829±1.8	0.808
SI012-5.1	368	499	1.40	26.4	—	516.8± 9.2	608±34	520±11	15	11.99±1.9	0.05980±1.5	11.98±1.9	0.06012±1.6	0.692±2.4	0.0835±1.9	0.766
SI012-6.1	540	566	1.08	39.2	0.19	521.8± 9.2	466±34	516±10	–12	11.84±1.8	0.05792±1.2	11.86±1.8	0.05634±1.6	0.655±2.4	0.0843±1.8	0.761
SI012-7.1	240	267	1.15	17.3	—	521.0± 9.5	484±46	517±12	–8	11.89±1.9	0.0562±1.9	11.88±1.9	0.05680±2.1	0.659±2.8	0.0842±1.9	0.672
SI012-8.1	373	612	1.70	26.8	0.27	517.6± 9.2	445±51	517±11	–16	11.93±1.8	0.05803±1.5	11.96±1.9	0.05580±2.3	0.643±2.9	0.0836±1.9	0.631
SI012-9.1	109	256	2.42	8.01	—	528.0±10	540±66	529±13	2	11.73±2.0	0.05710±2.7	11.72±2.0	0.05830±3.0	0.686±3.6	0.0853±2.0	0.559
SI012-10.1	319	537	1.74	23.6	—	533.7± 9.6	495±36	539±11	–8	11.59±1.9	0.05676±1.6	11.59±1.9	0.05710±1.6	0.679±2.5	0.0863±1.9	0.749
SI012-11.1	152	235	1.60	10.9	0.42	513.2± 9.6	360±65	509±12	–43	12.02±2.0	0.05710±2.3	12.07±2.0	0.05370±2.9	0.614±3.5	0.0829±2.0	0.559
SI012-12.1	139	291	2.16	9.91	0.46	511.6± 9.9	451±99	499±12	–13	12.05±2.0	0.05970±2.5	12.11±2.0	0.05600±4.4	0.637±4.9	0.0826±2.0	0.412
SI012-13.1	207	330	1.65	14.8	0.42	511.3± 9.4	342±66	511±11	–50	12.06±1.9	0.05680±2.0	12.11±1.9	0.05330±2.9	0.607±3.5	0.0826±1.9	0.549
SI012-14.1	392	604	1.59	27.9	0.14	511.2± 9.4	425±49	504±11	–20	12.10±1.9	0.05646±1.5	12.12±1.9	0.05530±2.2	0.629±2.9	0.0825±1.9	0.660
SI012-15.1	325	492	1.57	22.8	0.15	505.3± 9.1	415±47	494±10	–22	12.25±1.9	0.05626±1.7	12.26±1.9	0.05510±2.1	0.619±2.8	0.0815±1.9	0.664

Notes: Errors are 1-sigma; Pb_c and Pb* indicate the common and radiogenic portions, respectively; "—" means not detected. Error in standard calibration was 0.39% (not included in above errors but required when comparing data from different mounts). "(1)" Common Pb corrected using measured ^{204}Pb.

Seventeen zircon grains of this sample were analyzed and the results are listed in Table 1. The U concentrations vary between 106 and 1473 ppm, and the Th concentrations between 185 and 1151 ppm, with Th/U ratios from 0.41 to 2.61, which indicates the heterogeneity of the zircon grains and suggests a magmatic origin. Exclusion of the reversely discordant analysis spot 13.1 yielded a weighted mean $^{206}Pb/^{238}U$ age of 495.8±4.2 Ma (Figure 4a), which reflects the granite crystallization or emplacement age.

3.2 SHRIMP U-Pb geochronology of sample SI01-2

The morphology of zircons in this sample is similar to sample SI01-1, showing euhedral and anhedral shapes (Figure 3b). They have grain sizes ranging from *ca.* 100 to 600 μm. Most zircons present oscillatory or sector zoning, and again while some grains have evidence for a local intermediate stage of resorption, their morphology indicates that they crystallised from magma.

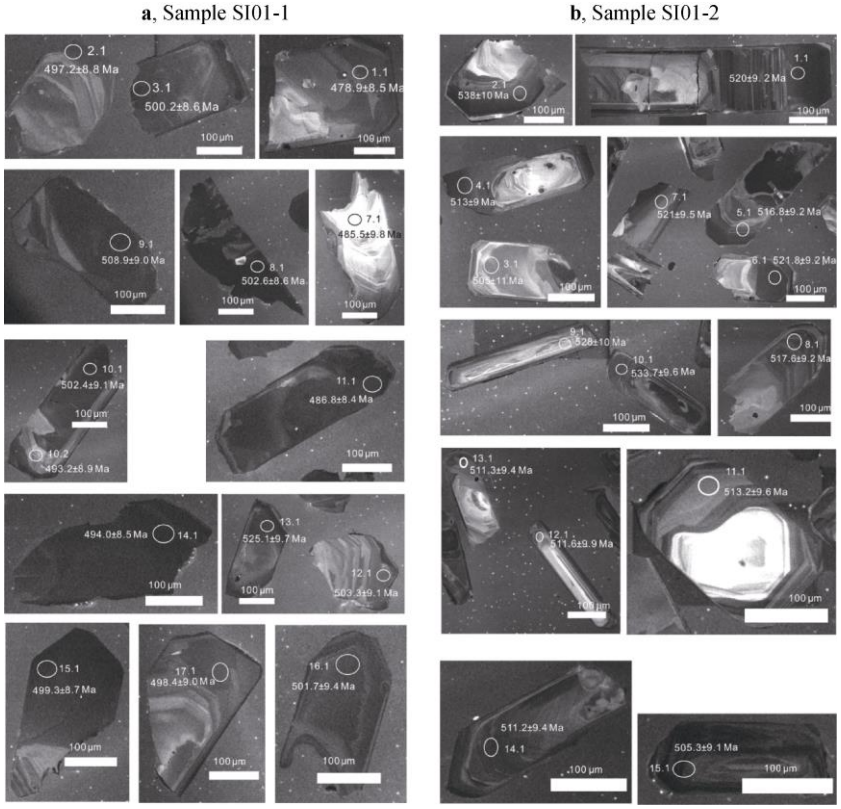

Figure 3 Cathodoluminescence (CL) images of zircons from the SIG. Ellipes represent SHRIMP spots annotated with analysis number and $^{206}Pb/^{238}Pb$ age (with 1 sigma error).

Fifteen zircons were analyzed and the results are also listed in Table 1. The U concentrations vary between 81 and 540 ppm, and the Th concentrations between 175 and 612 ppm, with Th/U ratios from 0.60 to 2.34, retaining typical magmatic values. Spot 2.1 has the oldest age of 538±10 Ma, and is slightly reversely discordant. Exclusion of spot 2.1 yielded a weighted mean $^{206}Pb/^{238}U$ age of 516±5 Ma (Figure 4b), which reflects the granite crystallization or emplacement age.

4 Discussion

4.1 The emplacement age of SIG

The SIG has not previously been dated to our knowledge. It has been always considered to have intruded simultaneously with the Landing Bluff Adamellite, a pink-grey coarse-grained porphyritic biotite granite with giant K-feldspar phenocrysts, and deformed xenoliths of gneissose biotite granodiorite (Sheraton et al., 1996; Tingey, 1981) that was emplaced during the Pan-African event (Tingey, 1991, 1981; Sheraton and Black,1988; Sheraton et al., 1984).

The SHRIMP U-Pb zircon geochronological data collected in this study provide new insight into the Sansom Island magmatism and its relationship with the Landing Bluff Granite. Our SHRIMP U-Pb zircon data for two granite samples from Sansom Island yield two ages, 495.8 ±4.2 Ma and 516±5 Ma, respectively. The prevailing view about pluton emplacement is that it is a relatively rapid process, taking less than 1 Ma (Wu et al., 2007; Petford et al., 2000). The notable age difference between our two samples indicates that the SIG was emplaced in two separate stages in the Cambrian, which is contrary to the previous assumption that this body formed at one time (Sheraton and Black, 1988; Tingey, 1981 and references

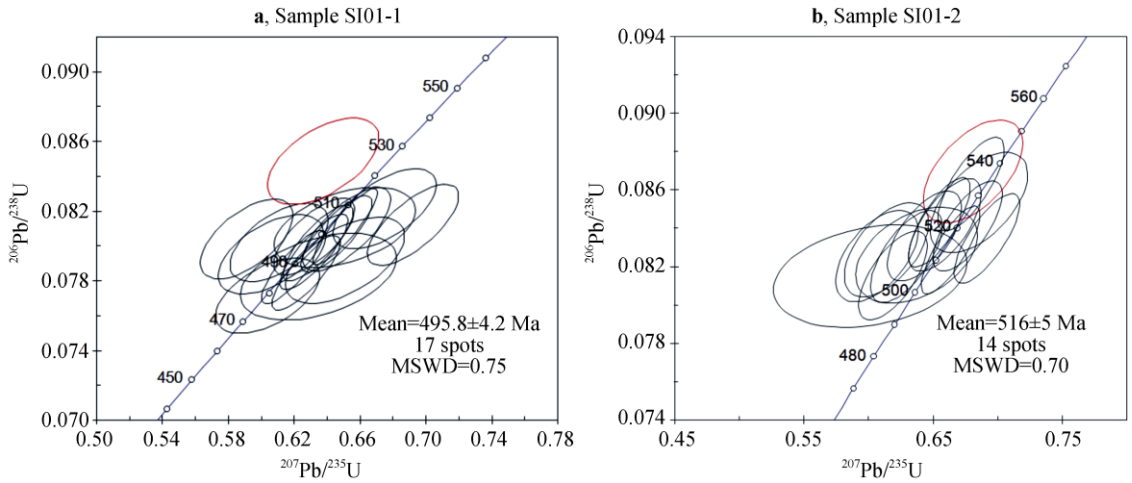

Figure 4 SHRIMP U-Pb concordia diagrams for zircons from the SIG (analyses plotted with ±1 sigma errors). Analyses excluded from weighted average calculations are indicated by red ellipses.

therein). Such episodic magmatic activity in one pluton can be found in many places worldwide, including the Manaslu Intrusive Complex in the Himalaya (Harrison et al., 1999) and the Tuolumne Intrusive Suite in California (Coleman et al., 2004).

4.2 Geological implication

SHIRMP U-Pb zircon dating of the SIG in this study supports the idea that rocks in Prydz Bay were affected by Pan-African events (Fitzsimons et al., 1997; Hensen and Zhou, 1995; Zhao et al., 1992). The Pan-African Prydz Belt extends along the coast of Prydz Bay, and then extends southward to the southern Prince Charles Mountains through the Amery Ice Shelf (Liu et al., 2009 and reference therein). It is a belt of Late Neoproterozoic/Cambrian magmatism, deformation and metamorphism. The period of magmatism can be divided into five phases (Figure 5), based on the new data presented here accompanied with previously published data. The oldest magmatic age of 706±285 Ma is reported at Mt. Stinear in the southern Prince Charles Mountains (Mikhalsky and Roland, 2007), but the very large error means this cannot be reliably distinguished from the more common 550−500 Ma ages. Magmatic ages of 550−530 Ma are obtained from Mt. Meredith, Rofe Glacier of the southern Prince Charles Mountains and the Grove Mountains (Gongurov et al., 2007; Mikhalsky and Roland, 2007; Liu et al., 2006), while *ca.* 525 Ma magmatism is not so common but is reported from the Grove Mountains, and Mt. McCauley of southern Prince Charles Mountains (Mikhalsky and Roland, 2007; Liu et al., 2006). Magmatic rocks aged *ca.* 515−520 Ma crop at several mounts/bluffs of the southern Prince Charles Mountains and Larsemann Hills (Li et al., 2007; Mikhalsky and Roland, 2007), whereas *ca.* 500 Ma magmatic activity is widespread in the Prydz Belt (Li et al., 2007; Mikhalsky and Roland, 2007; Liu et al., 2006). These granites can also be divided into two groups based on their deformation. Most of the granitic rocks are deformed, but undeformed granites crop out at Mt Meredith and in the Larsemann Hills area (Gongurov et al., 2007; Li et al., 2007; Wang et al., 2003; Zhao et al., 2003; Carson et al., 1996; Zhao et al., 1992). The *ca.* 515 Ma deformed granites in the Prydz Belt were synchronous with a high-grade transpressional event (D2) (Carson et al., 1996). These relationships suggest that there are regional variations in the deformation history.

Our data show that Sansom Island records two-stage magmatism, which is different from the single stage inferred from granites at Landing Bluff, suggesting that the Landing Bluff Adamellite is a composite body with a more complex evolution than believed previously. Granite from Landing Bluff is not deformed and was emplaced at about 500 Ma (Tingey, 1981), but it contains deformed xenoliths with a zircon age of 503±8 Ma (Mikhalsky and Roland, 2007). These ages date the deformation at Landing Bluff between 500 Ma and 503 Ma. This raises the question of why this deformation at Landing Bluff is not seen at Sansom Island. The most reasonable explanation is that the deformation seen in xenoliths at Landing Bluff is only of local extent and did not occur at Sansom Island, even though these two locations are close to one another. A detailed integrated study of petrogenesis and deformation in this region might help to resolve these uncertainties.

5 Conclusions

The SHRIMP U-Pb zircon geochronology was conducted on SIG to understand the emplacement time of it. The following conclusions are achieved:

(1) New SHRIMP U-Pb zircon isotopic data show that

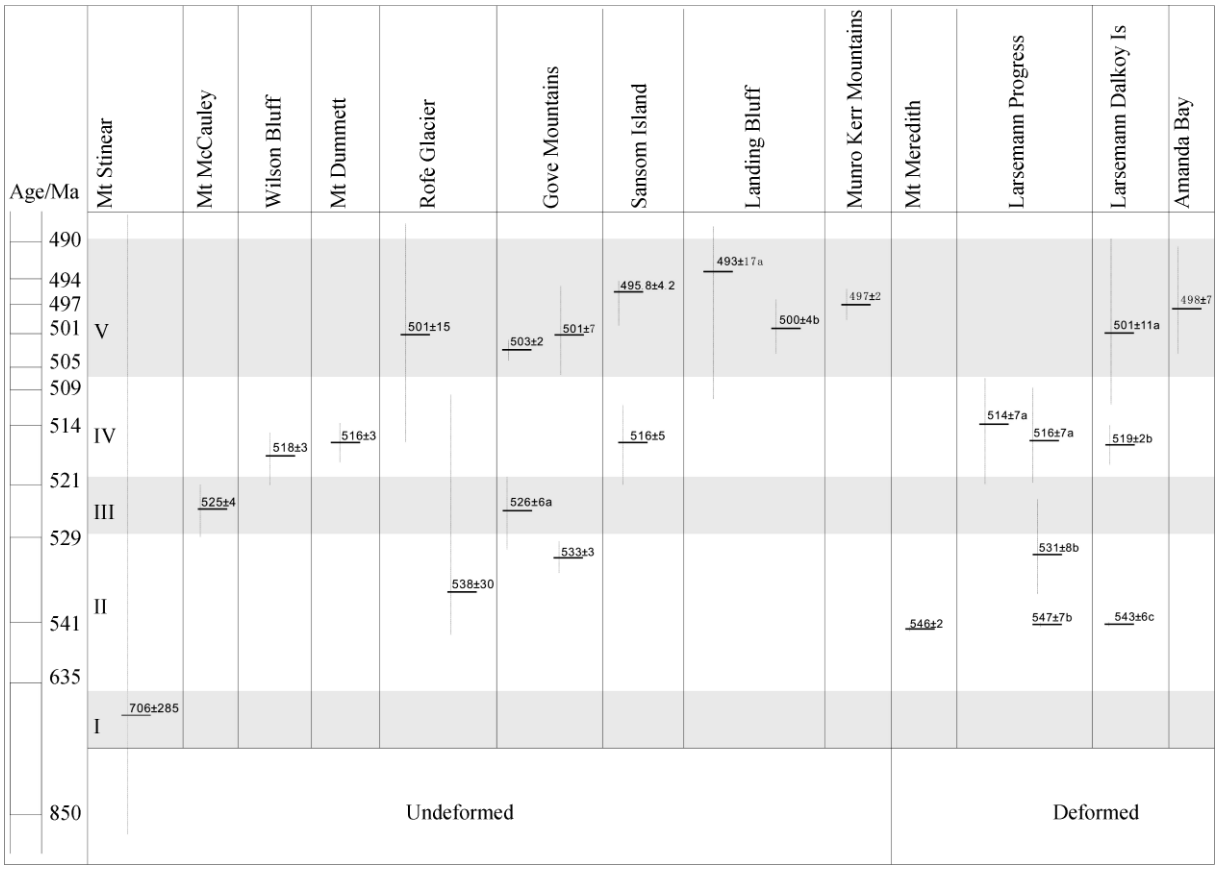

Figure 5 Time-space diagram for major Pan-African granitic bodies in the Amery Ice Shelf – Prydz Bay region. Five magmatic phases are divided based on the published age data (for detail see in text). The age scale is from Walker et al. (2012). References: the Mt Stinear granite, the Mt Dummett granite, the Mt McCauley granite, the Wilson Bluff granite and the Rofe Glacier granite are from Mikhalsky and Roland (2007); the Grove Mountains granite is from Liu et al. (2006), while age of 526±6 Ma is from Zhao et al. (2003); the Landing Bluff granite is from Tingey (1991); the Munro Kerr Mountains granite and the Amanda Bay granite are from Li et al. (2007); Mt Meredith granite is from Gongurov et al. (2007); the Larsemann Progress granite (a) is from Carson et al. (1996); the Larsemann Progress granite (b) is from Zhao et al. (1992); the Larsemann Dalkoy Island granite (a) is from Wang et al. (2003); the Larsemann Dalkoy Island granite (b) is from Li et al. (2007); the Larsemann Dalkoy Island granite (c) is from Zhao et al. (2003).

the SIG was emplaced in two episodes: 516±5 Ma and 495.8±4.2 Ma. These data challenge the traditional one-stage model for magmatism in this area and instead argue for a more complex history.

(2) The data indicate that Sansom Island is part of the Pan-African Prydz Belt, but also point to some discrepancies in local geology. In particular, the lack of deformation in the older *ca.* 516 Ma intrusion at Samson Island conflicts with evidence for gneissose xenoliths at nearby Landing Bluff dated at *ca.* 503 Ma. Detailed research on regional petrogenesis and deformation will improve our understanding of these events.

Acknowledgments Prof. Simon Harley, Prof. Ian Fitzsimons and an anonymous reviewer are thanked for their critical reviews that improved the manuscript. The fieldwork was conducted during the 31st CHINARE (2014/2015), and funded by the National Natural Science Foundation of China (Grant no. 41530209), the Chinese Polar Environment Comprehensive Investigation and Assessment Programs (Grant nos. CHINARE2015-02-05, CHINARE2017-04-03), the Taishan Scholar Project (Grant no. TSPD20161007) and the Fundamental Research Funds for National Public Research Institutes of China (Grant nos. 2009T02, 2014T01). Logistic support was provided by the Australian Antarctic Division and the Chinese Arctic and Antarctic Administration, SOA.

References

Black L P, Kamo S L, Allen C M, et al. 2003. TEMORA 1: a new zircon standard for Phanerozoic U-Pb geochronology. Chem Geol, 200(1-2): 155-170.

Boger S D, Wilson C J L, Fanning C M. 2001. Early Paleozoic tectonism within the East Antarctic craton: The final suture between east and west Gondwana? Geology, 29(5): 463-466.

Carson C J, Fanning C M, Wilson C J L. 1996. Timing of the progress granite, larsemann hills: additional evidence for early Palaeozoic orogenesis within the East Antarctic Shield and implications for Gondwana assembly. Aust J Earth Sci, 43(5): 539-553.

Coleman D S, Gray W, Glazner A F. 2004. Rethinking the emplacement and evolution of zoned plutons: geochronologic evidence for incremental assembly of the Tuolumne Intrusive Suite, California. Geology, 32(5): 433-436.

Corvino A F, Boger S D, Henjes-Kunst F, et al. 2008. Superimposed tectonic events at 2450 Ma, 2100 Ma, 900 Ma and 500 Ma in the North Mawson Escarpment, Antarctic Prince Charles Mountains. Precam Res, 167(3-4): 281-302.

Fitzsimons I C W. 2000. A review of tectonic events in the East Antarctic Shield and their implications for Gondwana and earlier supercontinents. J Afr Earth Sci, 31(1): 3-23.

Fitzsimons I C W. 1997. The Brattstrand Paragneiss and the Søstrene Orthogneiss: a review of Pan-African metamorphism and Grenvillian relics in southern Prydz Bay//Ricci C A. The Antarctic region: geological evolution and processes. Siena: Terra Antarctica Publications, 121-130.

Gongurov N A, Laiba A A, Beliatsky B V. 2007. Major magmatic events in Mt Meredith, Prince Charles Mountains: first evidence for early Palaeozoic syntectonic granites//Cooper A K, Raymond C R. Antarctica: A keystone in a changing world–Online Proceedings of the 10th ISAES. USGS Open-File Report 2007–1047, Short Research Paper 100. Reston, VA: U.S. Geological Survey, 4, doi: 10.3133/of2007-1047.srp100.

Harrison T M, Grove M, Mckeegan K D, et al. 1999. Origin and episodic emplacement of the Manaslu Intrusive Complex, Central Himalaya. J Petrol, 40(1): 3-19.

Hensen B J, Zhou B. 1995. A Pan-African granulite facies metamorphic episode in Prydz Bay, Antarctica: evidence from Sm-Nd garnet dating. Aust J Earth Sci, 42(3): 249-258.

Hokada T, Harley S L, Dunkley D J, et al. 2016. Peak and post-peak development of UHT metamorphism at Mather Peninsula, Rauer Islands: zircon and monazite U-Th-Pb and REE chemistry constraints. J Mineral Petrol Sci, 111(2): 89-103.

Li M, Liu X C, Zhao Y. 2007. Zircon U-Pb ages and geochemistry of granitoids from Prydz Bay, East Antarctica, and their tectonic significance. Acta Petrol Sin, 23(5): 1055-1066 (in Chinese).

Liu J, Zhao Y, Liu X C, et al. 2011. Multiple deformations in the Reinbolt Hills of the eastern Amery Ice Shelf, East Antarctica, and their tectonic implications. Chin J Polar Res, 23(4): 299-309 (in Chinese with English abstract).

Liu X C, Jahn B M, Zhao Y, et al. 2014. Geochemistry and geochronology of Mesoproterozoic basement rocks from the eastern Amery Ice Shelf and Southwestern Prydz Bay, East Antarctica: implications for a long-lived magmatic accretion in a continental arc. Amer J Sci, 314(2): 508-547.

Liu X C, Jahn B M, Zhao Y, et al. 2006. Late Pan-African granitoids from the Grove Mountains, East Antarctica: age, origin and tectonic implications. Precam Res, 145(1-2): 131-154.

Liu X C, Zhao Y, Song B, et al. 2009. SHRIMP U-Pb zircon geochronology of high-grade rocks and charnockites from the eastern Amery Ice Shelf and southwestern Prydz Bay, East Antarctica: constraints on Late Mesoproterozoic to Cambrian tectonothermal events related to supercontinent assembly. Gondwana Res, 16(2): 342-361.

Liu X C, Zhao Y, Zhao G C, et al. 2007. Petrology and geochronology of granulites from the McKaskle Hills, eastern Amery Ice Shelf, Antarctica, and implications for the evolution of the Prydz Belt. J Petrol, 48(8): 1443-1470.

Ludwig K R. 2003. User's manual for Isoplot 3.00: a geochronological toolkit for Microsoft excel. Berkeley CA: Special Publication, 4.

Ludwig K R. 2001. SQUID 1.02: A User's Manual. Berkeley Geochronology Center. Berkeley CA: Special Publication, 2.

Mikhalsky E V, Roland N W. 2007. New data on the age and geochemical features of granites in the southern Prince Charles Mountains and Prydz Bay Coast. Terra Antarct, 14(1): 43-60.

Moores E M. 1991. Southwest U.S.–East Antarctic (SWEAT) connection: a hypothesis. Geology, 19(5): 425-428.

Nichols G T, Berry R F. 1991. A decompressional *P-T* path, Reinbolt Hills, East Antarctica. J Metamorph Geol, 9(3): 257-266.

Petford N, Cruden A R, Mccaffrey K J W, et al. 2000. Granite magma formation, transport and emplacement in the Earth's crust. Nature, 408(6813): 669-673.

Phillips G, Kelsey D E, Corvino A F, et al. 2009. Continental reworking during overprinting orogenic events, southern Prince Charles Mountains, East Antarctica. J Petrol, 50(11): 2017-2041.

Sheraton J W, Black L P. 1988. Chemical evolution of granitic rocks in the East Antarctic Shield, with particular reference to post-orogenic granites. Lithos, 21(1): 37-52.

Sheraton J W, Black L P, Mcculloch M T. 1984. Regional geochemical and isotopic characteristics of high-grade metamorphics of the Prydz Bay area: the extent of Proterozoic reworking of Qrchaean continental crust in East Antarctica. Precam Res, 26(2): 169198.

Sheraton J W, Tindle A G, Tingey R J. 1996. Geochemistry, origin, and tectonic setting of granitic rocks of the Prince Charles Mountains, Antarctica. AGSO J Aust Geol and Geophys, 16: 345370.

Stacey J S, Kramers J D. 1975. Approximation of terrestrial lead isotope evolution by a two-stage model. Earth Planet Sci Lett, 26(2): 207-221.

Stüwe K, Braun H M, Peer H. 1989. Geology and structure of the Larsemann Hills area, Prydz Bay, East Antarctica. Aust J Earth Sci, 36(2): 219-241.

Stüwe K, Powell R. 1989. Low-pressure granulite facies metamorphism in the Larsemann Hills area, East Antarctica: petrology and tectonic implications for the evolution of the Prydz Bay area. Metamorph Geol, 7(4): 465-483.

Tingey R J. 1981. Geological investigations in Antarctica 1968–1969: the Prydz Bay–Amery Ice Shelf–Prince Charles Mountains area. Australia, Canberra: Bureau of Mineral Resources, 1-72.

Tingey R J. 1991. The regional geology of Archaean and Proterozoic rocks in Antarctica//Tingey R J. The geology of Antarctica. Oxford: Oxford University Press, 1-73.

Walker J D, Geissman J W, Bowring S A, et al. 2012. Geologic time scale (v.4.0). Geological Society of America, doi: 10.1130/2012.CTS004R3C.

Williams I S. 1998. U-Th-Pb geochronology by ion microprobe// Mckibben M A, Shanks W C, Ridley W I. Applications of microanalytical techniques to understanding mineralizing processes. Reviews in Economic Geology, Vol. 7. Littleton: Society of Economic Geologists, 1-35.

Wilson C J L, Quinn C, Tong L X, et al. 2007. Early Palaeozoic intracratonic shears and post-tectonic cooling in the Rauer Group, Prydz Bay, East Antarctica constrained by $^{40}Ar/^{39}Ar$ thermochronology. Antarct Sci, 19(3): 339-353.

Wu F Y, Li X H, Yang J H, et al. 2007. Discussions on the petrogenesis of

granites. Acta Petrol Sin, 23(6): 1217-1238 (in Chinese).

Zhao Y, Liu X H, Liu X C, et al. 2003. Pan-African events in Prydz Bay, East Antarctica and its inference on East Gondwana tectonics// Yoshida M, Windley B, Dasgupta S. Proterozoic East Gondwana: Supercontinent Assembly And Breakup. London: Geological Society, Special Publications, 231-245.

Zhao Y, Song B, Wang Y, et al. 1992. Geochronology of the late granite in the Larsemann Hills, East Antarctica//Yoshida Y, Kaminuma K, Shiraishi K. Recent progress in Antarctic Earth Science. Tokyo: Terra Scientific Publishing Company, 155-161.